PCCP

ARTICLE

Unravelling the nature of glyphosate binding to goethite surfaces by ab initio molecular dynamics simulations

Ashour A. Ahmed,[*a,b] Peter Leinweber[c] and Oliver Kühn[a]

Received 00th January 20xx,
Accepted 00th January 20xx

DOI: 10.1039/x0xx00000x

www.rsc.org/

Investigation of the interaction between glyphosate (GLP) and soil minerals is essential for understanding GLP's fate in the environment. Whereas GLP–goethite binding has been discussed extensively, the impact of water as well as of different goethite surface planes has not been studied yet. In this contribution, periodic density functional theory-based molecular dynamics simulations are applied to explore possible binding mechanisms for GLP with three goethite surface planes (010, 001, and 100) in the presence of water. The investigation included several binding motifs of monodentate (**M**) and bidentate (**B**) type. It was found that the binding stability increasing in the order **M**@001 < **M**@010 < 2O+2Fe **B**@100 < **M**@100 < 1O+2Fe **B**@001 < 2O+1Fe **B**@010. This behavior has been traced to the presence of intramolecular H-bonds (HBs) in GLP, intermolecular HBs between GLP and water, GLP and goethite, and water and goethite. These interactions are accompanied by proton transfer from GLP to water and to goethite, and from water to goethite as well as water dissociation at the goethite surface. Further, it was observed that OH^- species can replace the adsorbed GLP at the goethite surface, which could explain the well-known drastic drop in the GLP adsorption at high pH. The present results highlight the role of water in the GLP-goethite interaction and provide a molecular level prospect on available experimental data.

1. Introduction

There is an ongoing debate about the use of glyphosate (GLP, N-(phosphonomethyl)-glycine) in view of its possible carcinogenic effects[1,2] and its occurrence in ground and surface water [3,4], for instance, in the Baltic Sea[5]. GLP is the most widely used nonselective post-emergent herbicide in the world. It is applied to many food and non-food crops as well as non-crop areas such as roadsides.[6] It has a highly polar character due to its three polar functional groups (amino, carboxylic, and phosphonic groups, see Fig. 1). As a consequence of its chemical properties, GLP is strongly bound to soil constituents, highly soluble in water, and charged according to the soil pH.[7] Due to the chemical similarity between the GLP phosphonate group and inorganic phosphates, they compete with each other for the same sorption sites at soil components.[8,9]

In soil, GLP binds to heavy metals,[6,10] soil organic matter (SOM),[11,12] and soil minerals[13,14]. The strong binding to mineral surfaces is commonly taken as an important factor for the deactivation of GLP in soil,[15,16] which leads to a reduction of its mobility and herbicide efficiency[17,18]. Consequently, understanding the nature and extent of the interaction of GLP with soil mineral surfaces is a key point for investigation of the impact and fate of GLP in the environment. Previous experimental studies showed strong adsorption for GLP on soil-abundant mineral surfaces of gibbsite (α-$Al(OH)_3$),[17] bayerite (β-$Al(OH)_3$),[19] manganite (γ-MnOOH),[20] and goethite (α-FeOOH)[21–25].

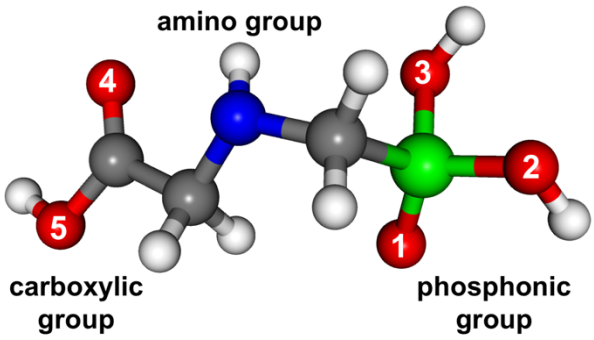

Figure 1. GLP spatial configuration with its three polar (amino, carboxylic, and phosphonic) functional groups. White, gray, blue, red, and green colors are corresponding to H, C, N, O, and P atoms, respectively. Its five oxygen atoms are labelled with numbers from 1 to 5 to aid the discussion of the GLP–goethite–interaction.

Particularly, the mineral goethite received much attention over the past few decades because it is the most common ferric iron Fe(III) oxyhydroxide in soils and its reactivity couples to a wide range of environmental processes. Sheals et al.[23] and Barja and Afonso[24] both showed that the GLP adsorption on goethite surface decreases with increasing the soil pH. Sheals et al.[23] employed adsorption batch experiments, infrared and photoelectron spectroscopy to find evidence for the formation

[a] University of Rostock, Institute of Physics, D-18059 Rostock, Albert-Einstein-Str. 23-24, Germany. Email: ashour.ahmed@uni-rostock.de
[b] University of Cairo, Faculty of Science, Department of Chemistry, 12613 Giza, Egypt.
[c] University of Rostock, Soil Science, D-18059 Rostock, Germany.
† Electronic Supplementary Information (ESI) available: [details of any supplementary information available should be included here]. See DOI: 10.1039/x0xx00000x

of intramolecular hydrogen bonds (HBs) between the GLP amino group and both the carboxylate and the phosphonate groups at low pH. This HB is lost upon deprotonation of the amino group at high pH. In another experimental study, it was observed that the amino and carboxylic functional groups do not contribute to the surface complexation.[24] In contrast, the GLP phosphonate group was found to bind directly to the goethite surface, forming inner-sphere complexes via predominantly monodentate (**M**) complexation. This **M** form was supported by a quantum mechanical study using a cluster model.[26] Furthermore, the formation of a minor quantity of bidentate (**B**) complexes is possible at low GLP surface coverage and around neutral pH. Barja and Afonso[24] indicated that GLP adsorbs on goethite surface through the phosphonate group in a **B** form at pH range of 3.5–9.2 and low to moderate surface coverage, and in a **M** form at low pH and high surface coverage. Moreover, they reported that the GLP phosphonate group of the **B** complex is unprotonated, and that of the **M** complex is mostly protonated. Despite these studies, systematic knowledge about the dynamics and mechanism of the GLP–goethite interaction at the molecular level is still lacking. In particular, there are neither experimental nor theoretical studies focusing on the overall GLP–goethite–water interactions and the individual (GLP–goethite, GLP–water, and goethite–water) interactions for different goethite surface planes at a molecular scale.

The main objective of the present contribution is to unravel the nature of binding between GLP and different goethite surface planes at the molecular level by means of periodic density functional theory (DFT) based molecular dynamics (MD) simulations. Specifically, mixed Gaussian and plane wave calculations will be performed for investigation of the interaction of GLP with three different goethite surface planes in the presence of water. Based on previous experimental outcomes,23,24 only binding of GLP through its phosphonate group with the goethite surfaces will be considered. The individual GLP–goethite, GLP–water, and goethite–water interactions will be addressed. Further, the competition between GLP and water molecules for adsorption sites will be explored. The present exhaustive study of different binding motifs and surface planes using a state-of-the-art computational approach provides a benchmark and starting point for future investigations of interactions of GLP with soil constituents.

2. Molecular modelling and computational details

2.1. Model systems

In order to investigate possible binding motifs between GLP's phosphonate group and goethite, three different goethite surface planes (010, 001, and 100 according to the Pnma space group) were considered. These three goethite surface planes have been selected due to the prominent stability of the 010 surface[27,28] and the abundance of the 100 and 001 surfaces[29–33]. Moreover, these three surfaces exhibit three kinds of Fe atoms with three different coordination numbers based on the surface plane. In view of the heterogeneity of mineral particles, the present models resemble typical binding situations, but without considering the aspect of imperfections. The three model surfaces were described by periodic slabs, constructed by repetition of the goethite unit cell[34] shown in Fig. 2a in the relevant directions. The goethite orthorhombic unit cell contains four FeOOH formula units (16 atoms, lattice constants are a = 9.9560 Å, b= 3.0215 Å, and c = 4.6080 Å). The 010, 001, and 100 goethite surface planes were generated from 2a × 2b × 2c (Fig. 2b), 2a × 4b × 1c (Fig. 2c), and 1a × 4b × 3c (Fig. 2d) unit cells, respectively. To simulate these surfaces, a layer of about 20 Å vacuum was added between the periodic slabs perpendicular to the surface plane. GLP was added to the vacuum region with its long axis being perpendicular to the surface planes such as to facilitate binding through the phosphonate group. For each surface plane, GLP was situated in two starting spatial configurations to construct **M** and **B** motifs between the phosphonate O atoms and the goethite Fe atoms. Due to the expected importance of solvating water for the GLP–surface interaction, water molecules at a density of about 1g/cm^3 were introduced into the vacuum region between the slabs to construct the final simulation box (for example, see Fig. 2e, which contains 128 FeOOH atoms + 1 GLP molecule + 84 water molecules = 398 atoms). The solvation procedure involved filling the box vacuum region with a generic equilibrated 3-point water solvent model (SPC), by using the solvation tool provided by the GROMACS package [35]. Hence, in total there are six GLP–goethite–water models, i.e. **M** and **B** at each of the three surface planes. For each model, the bottom layer atoms of the relevant goethite surface plane were kept fixed to approximate the properties of the underlying extended goethite bulk and to decrease the interaction with water of the next box image.

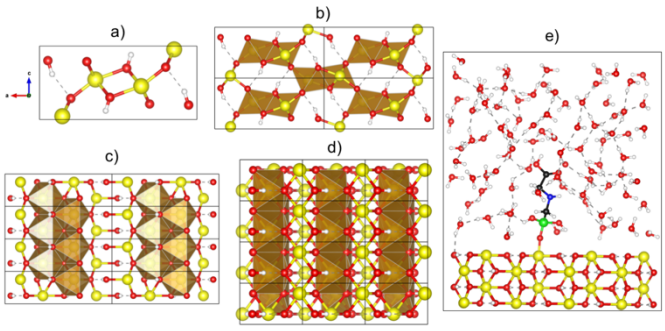

Figure 2. Goethite unit cell (a), top view for the modelled goethite surface planes 010 (b), 001 (c), and 100 (d) in the Pnma space group using a polyhedral representation, and GLP–goethite (010)–water model (e). The polyhedra represent Fe in octahedral coordination. White, black, blue, red, green, and yellow colours are corresponding to H, C, N, O, P, and Fe atoms, respectively.

2.2. Quantum chemical calculations

For the six GLP–goethite–water models, DFT-based Born–Oppenheimer MD simulations have been carried out using the quickstep code[36] implemented in the CP2K simulation package[37]. Here, the hybrid Gaussian and plane-wave (GPW) method[38] was applied for calculating the DFT electronic ground

state structure. The Perdew–Burke–Ernzerhof functional (PBE)[39] has been used together with the Goedecker–Teter–Hutter (GTH) pseudopotentials[40]. The electronic density cutoff for atomic core electrons was chosen as 500 Ry. The double–ζ valence polarized (DZVP) basis set optimized for the GTH pseudopotentials[41] has been used for all atomic species included in GLP and the goethite surface model. For O and H atoms of water, the corresponding single–ζ valence (SZV) basis set has been applied to reduce the computational cost. The empirical dispersion correction D3 by Grimme et al.[42] was employed. Periodic boundary conditions have been applied in all the three spatial directions. Moreover, the total energy value was tuned to be accurate up to 10^{-10} with a convergence threshold for the SCF energy of 10^{-5}. 25 picoseconds (ps) NVT-MD simulations have been performed for each model with a time step of 0.5 femtoseconds (fs) for integrating the equations of motion. The temperature was kept at 300 K through a velocity rescaling thermostat (canonical sampling through velocity rescaling, CSVR) with time constant of 100 fs and temperature tolerance of 10 K. Based on analysis of potential energy, kinetic energy, and temperature, the first 10 ps were assigned for equilibration, the remaining 15 ps (production trajectories) were analysed in terms of dynamics of the individual GLP–goethite–, GLP–water–, and goethite–water–interactions.

To characterize the complexation reaction, GLP + goethite surface ➔ GLP–goethite–complex, snapshots are taken every 50 fs during the production trajectories. For each snapshot, the interaction energy (E_{int}) between GLP and each goethite surface plane for this complexation reaction was calculated as follows:

$$E_{int} = E_{\text{GLP–goethite–complex}} - (E_{\text{GLP}} + E_{\text{goethite surface}}) \qquad (1)$$

where, $E_{\text{GLP–goethite–complex}}$, E_{GLP}, and $E_{\text{goethite surface}}$ are the total electronic energy of the GLP–goethite–complex, GLP, and goethite surface, respectively. Here, the effect of the basis set superposition error (BSSE) has been corrected using the counterpoise scheme.[43]

To investigate the effect of water on the GLP–goethite–interaction, a MD simulation has been performed for one of the GLP–goethite models in vacuum. Here, the same initial configuration for GLP on top of the 010 goethite surface plane in presence of water (Fig. 2e) was selected but without including water. The same box dimensions and all MD parameters have been used exactly as in the water case. Moreover, geometry optimization has been performed for the same six GLP–goethite models mentioned above at the same level of theory and with the same parameters as used in the MD simulations, but without including water.

3. Results and discussion

In the goethite bulk, each Fe atom is surrounded by six O atoms (three O^{2-} and three OH^-) to give $FeO_3(OH)_3$ octahedra. For the bare goethite surface, coordination of the surface Fe atoms with the neighbouring O atoms depends on the surface plane. Here, we will discuss three different planes having three different Fe coordination numbers. Specifically, each surface Fe atom is coordinated by three, four, and five O atoms for the 001, 010, and 100 goethite surface planes, respectively (see Fig. 2b-d). For this reason, the nature and mechanism of the GLP–goethite interaction as well as water–goethite interaction depend on the goethite surface plane. In the following this dependence will be explored on the basis of MD simulations. Important average bond lengths and interaction energies are summarized in Tab. 1.

3.1. Glp @ 010 surface plane

Regarding the GLP–goethite–interaction, at the 010 surface plane Fe atoms may exhibit two different binding motifs, i.e. **M** and **B**. At the 010 surface plane, the shortest and longest distances between the adjacent Fe atoms are around 4.6 and 5.4 Å, respectively. Therefore, formation of **B** complex between GLP and this surface plane will mainly take place between two GLP phosphonate O atoms and one Fe atom.

3.1.1. Monodentate (M) binding motif

For the **M** motif, GLP was set initially close to a central surface Fe atom through its non-protonated oxygen (O1) of the phosphonate group. In course of the MD equilibration, chemical bond formation occurred between GLP and goethite, water and goethite, and GLP and water.

Regarding the GLP–goethite interaction, a stable **M** complex has been formed between GLP and the goethite surface (see Fig. 3a). Along the production trajectory, the length of the **M** Fe-O1 covalent bond ranges from 1.83 to 2.12 Å with an average of 1.96 Å (see Fig. S1a in the supplementary information (SI)). The distances between the same Fe atom and the other phosphonate O atoms (O2 and O3) vary in the range of 3.32–3.80 and 3.61–4.16 Å giving rise to averages of 3.56 and 3.93 Å, respectively. The distance between the phosphonate's P atom and the closest Fe atom changes from 3.02 to 3.36 Å with an average of 3.20 Å. Moreover, three proton (H^+) transfer processes have been observed from GLP to the goethite surface as well as to water (see Fig. 3a). Here, one proton is transferred from GLP to the goethite surface forming a strong HB (1.49 Å) with its original donating GLP O2 atom (see Fig. 3a and Fig. S2 in SI). This HB enhances formation of the **M** complex between GLP and the goethite surface and retards formation of the corresponding **B** one. For the other two proton transfer processes from GLP to water, both protons show HBs with their original donating GLP O3 and O5 atoms with average H---O distances of 1.86 and 1.89 Å (see Fig. 3a and Fig. S2b-c in SI). Moreover, it was observed that the GLP amino group through its H atom can form two bifurcated[44] weak intramolecular HBs with two O atoms (one from the phosphonic and one from the carboxylic group with average H---O distances of 2.52 and 2.50 Å, respectively). In general, these observations are in accord with experimental infrared spectra, which indicated that the GLP amino group forms two intramolecular HBs with the GLP phosphonic and carboxylic groups at low pH.[23] This enhances the possibility of formation of the **M** complex compared to the **B** complex.[23]

Regarding the water–goethite interaction, four water molecules approach the goethite surface along the MD simulation and

form four **M** binding motifs through their O atoms (O_{H_2O}) with the goethite surface Fe atoms (see Fig. S1b in SI). Their average Fe–O_{H_2O} bond lengths are in the range of 1.86–1.99 Å. Further, two of these four water molecules dissociate at the goethite surface producing two protons (H^+), which transfer to the goethite surface O atoms (O_{FeOOH}) forming covalent bonds. In addition, regardless of the covalent bond formation, water forms five HBs with goethite surface O atoms (see Fig. S1c in SI) and four HBs with GLP.

Next, let us have a quantitative picture of the strength of the GLP–goethite, water–goethite, and GLP–water interactions. Along the production trajectory, the interaction energy between GLP and goethite fluctuates around –110 kcal/mol (for details, see Fig. S3 in SI). The average energies along the trajectory for the interaction of 84 water molecules with GLP and goethite are –389 and –1710 kcal/mol, respectively. This indicates a very strong interaction between these three subsystems and shows that the water–goethite interaction is stronger than the water–GLP interaction. Recalculating these energies per single water molecule yields interaction energies of –4 and –20 kcal/mol for the water–GLP and water–goethite interaction, respectively, under the strong assumption of equal contributions for the water molecules regarding their interaction with GLP and goethite.

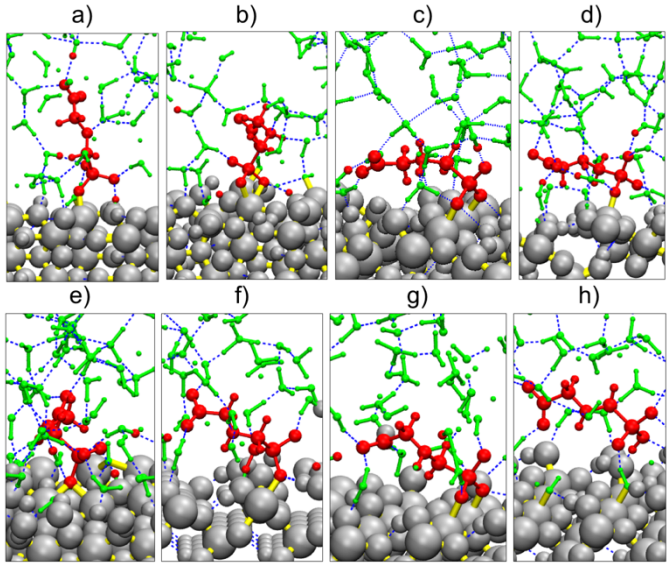

Figure 3. Snapshot along the equilibrated GLP–goethite–water trajectory for the **M** motif at the 010 goethite surface plane (a), 2O+1Fe **B** motif at the 010 surface plane (b), 2O+2Fe **B** motif at the 001 surface plane (c), **M** motif at the 001 surface plane (d), 1O+2Fe **B** motif at the 001 surface plane (e), **M** motif at the 100 surface plane (f), 2O+2Fe **B** motif at the 100 surface plane (g), and outer-sphere complex at the 100 surface plane (h). GLP, goethite, and water atoms are coloured in red, silver, and green, respectively. Intramolecular and intermolecular covalent bonds included goethite atoms are coloured in yellow and HBs are coloured in blue.

Table 1. Average interaction energies and selected distances obtained from the MD production trajectory for the different modelled binding motifs at the 010, 001, and 100 goethite surface planes.

surface plane	binding motif	E_{int} [kcal/mol]	distance [Å]			
			C–N	C–P	$Fe_{goethite}$–O_{GLP}	Fe–P
010	**M**	-110	1.47	1.85	1.96	3.20
	B (2O+1Fe)	-268	1.48	1.83	2.06 & 2.20	2.64
001	**M**	-68	1.49	1.83	2.02	3.36
	B (1O+2Fe)	-172	1.46	1.85	1.94 & 1.99	3.02 & 3.35
100	**M**	-154	1.47	1.83	2.04	3.28
	B (2O+2Fe)	-131	1.47	1.85	2.04 & 2.10	3.10 & 3.21

3.1.2. Bidentate (B) binding motif

In this case GLP was initially placed in a **B** motif between its phosphonate group and the 010 goethite surface. Similar to the **M** motif case, one observes a stable **B** complex formation in water. Here, the **B** complex is formed between two phosphonate O atoms (O1 and O2) and one surface Fe atom (2O+1Fe) as shown in Fig. 3b. The lengths of these two covalent bonds (Fe–O1 and Fe–O2) forming the **B** motif fluctuate around 2.06 and 2.20 Å. This means that each of these bonds is longer than the **M** Fe-O bond (1.96 Å). The average distance between the third phosphonate O atom and this Fe atom, participating in the **B** motif, (Fe–O3) is 3.56 Å. Here, the GLP phosphonate P atom is closer to the same Fe atom compared to the **M** case, with an average Fe–P distance of 2.64 Å. Furthermore, two protons are transferred from the GLP phosphonate group to the goethite surface O_{FeOOH} atoms (see Fig. 3b). These protons form HBs with their original donating O atoms (O2 and O3) with average H---O bond lengths of 1.79 and 2.48 Å. In addition, a proton transfer occurs from the GLP carboxylic O5 atom to the surrounding water (see Fig. 3b). Compared to the **M** case, the GLP amino group forms weaker intramolecular HBs with the phosphonic group, with an average H---O distance of 2.64 Å. Regarding the water–goethite interaction, **M** complexes between water O_{H_2O} atoms and the surface Fe atoms, water dissociation into H^+ and OH^- at the surface, proton transfer from water to the surface, and HBs between water and the surface are observed along the MD trajectory. Further, HBs between water and GLP are found as well. Finally, the average interaction energy between GLP and goethite for this **B** binding motif is –268 kcal/mol (see Fig. S3 in SI). This value is more than twice the value obtained for the **M** case due to formation of two Fe–O bonds in a cyclic form, the proton transfer from GLP to water and the surface, and saturation of the **B** Fe atom to its octahedral coordination. This indicates to a favoured formation of the **B** motif as compared with the **M** one. Finally, observation of the formation and stability of this 2O+1Fe **B** binding motif at the 010 goethite surface is in good agreement with the

experimental outcomes suggesting formation of the same binding motif.[23,24]

3.2. GLP @ 001 surface plane

For the 001 goethite surface plane, the shortest distance between any two adjacent surface Fe atoms is around 3.0 Å. Therefore, in principle this plane may exhibit **M** and **B** (2Fe atoms + 2 GLP O atoms) binding motifs for GLP at the surface. In the following, we will discuss the MD simulation results for two different starting configurations.

3.2.1. Monodentate (M) binding motif

For this case, the initial spatial configuration was actually set as a 2O+2Fe **B** motif for GLP at the 001 goethite surface plane. During the first three picoseconds of the MD trajectory, a 2O+2Fe **B** binding motif (see Fig. 3c) transiently existed, which eventually was disrupted to yield a stable **M** binding motif (1O+1Fe, see Fig. 3d). For this **M** motif, the average interaction energy between GLP and goethite is –68 kcal/mol (see Fig. S3 in SI). Here, the average distances of the **M** Fe–O and Fe–P bonds are 2.02 and 3.36 Å, respectively. Moreover, the GLP amino group forms two weak intramolecular HBs with the carboxylic and phosphonic groups. In addition, three protons are transferred from GLP to the surrounding water but stayed in contact via HBs with the GLP O2 and O5 atoms (see Fig. 3d).

Focusing on the water interaction with goethite and GLP, **M** complexes between water O atoms and the Fe surface atoms, water dissociation at the surface, proton transfer from water to the surface, and intermolecular HBs between water and the surface, and between water and GLP have been found along the MD trajectory.

3.2.2. Bidentate (B) binding motif

Starting with a **M** motif for GLP at the 001 goethite surface plane the configuration turned into a **B** one during the first picoseconds of the MD trajectory. It connects one GLP O atom (O1) in an oxonium fashion with two goethite Fe (Fe1 and Fe2) atoms (1O+2Fe, see Fig. 3e) that has not been discussed previously. The average interaction energy between GLP and goethite for this 1O+2Fe **B** motif is –172 kcal/mol (see Fig. S3 in SI). This indicates that the 1O+2Fe **B** binding motif is more stable than the **M** one at the 001 goethite surface plane. The average bond lengths for the two Fe1–O1 and Fe2-O1 bonds are 1.94 and 1.99 Å. The average distances between the GLP P atom and Fe1 and Fe2 atoms involved in the **B** motif are 3.02 and 3.35 Å. Moreover, two protons are transferred from the GLP O3 and O5 atoms to the surrounding water and a third one from the GLP O2 atom to the goethite surface (see Fig. 3e). Two of them form HBs with their original donating GLP O atoms (O2 and O5) with an average H---O bond lengths of 1.65 and 1.74 Å. In addition, the GLP amino group forms an intramolecular HB with the carboxylic one with an average H---O bond length of 2.41 Å.

Compared to the **M** motif at the 001 surface plane, here the same mechanism for the proton transfer processes from GLP to the goethite surface and surrounding water is effective. In addition, similar GLP–goethite–water interactions are found, involving intermolecular GLP–water HBs, goethite–water HBs, goethite(Fe)–(O)water covalent bonds in **M** and 1O+2Fe **B** forms, water dissociation at the surface, and proton transfer from water to the surface.

3.3. GLP @ 100 surface plane

The distance between the adjacent surface Fe atoms for this surface plane is exactly the same like for the 001 goethite surface plane. Therefore, this plane may exhibit **M** and **B** (2Fe atoms + 2 GLP O atoms) binding motifs for GLP at the surface. For this surface plane, each surface Fe atom is surrounded by 5 O atoms that means that the upper surface layer contains O atoms and not Fe atoms. This already indicates that it could be difficult for GLP to approach the surface Fe atoms through its phosphonic O atoms. For this reason, three cases will be discussed below involving **M,** and **B** and outer-sphere complex formation with the 100 goethite surface plane.

3.3.1. Monodentate (M) binding motif

We have observed a stable **M** motif for GLP at the 100 goethite surface plane along the MD trajectory (see Fig. 3f). Here, the average Fe–O1 bond length is 2.04 Å and the average distances between this Fe atom and the unbounded phosphonate O atoms (O2 and O3) are 3.54 and 4.52 Å. Further, the average distances of the Fe–P bond is 3.28 Å. Similar to the previous cases, proton transfer processes from the GLP to the surrounding water and goethite surface, formation of intramolecular HBs between GLP amino group and carboxylic group, and formation of goethite–water HBs have been observed. In contrast, the processes involving goethite(Fe)–(O)water covalent bonds, water dissociation at the surface, and proton transfer from water to the surface are not found for this case. Finally, the average interaction energy between GLP and goethite for this **M** motif is –154 kcal/mol (see Fig. S3 in SI).

3.3.2. Bidentate (B) binding motif

Starting with the **B** motif for GLP at the 100 goethite surface plane, we have observed almost the same reactions between the individual subsystems (GLP–goethite, GLP–water, and goethite–water) along the MD trajectory compared to the **M** motif at 100 surface plane. The only difference is that we have in this case a 2O+2Fe **B** motif with 2 GLP O atoms + 2 goethite Fe atoms (Fe1 and Fe2 see Fig. 3g). Here, the relevant average distances for the 2O+2Fe **B** motif are 2.04 (Fe1–O1), 2.10 (Fe2–O2), 2.57 (O1–O2), 2.95 (Fe1–Fe2), 3.10 (Fe1–P), and 3.21 Å (Fe2–P). The average interaction energy between GLP and the 100 goethite surface plane for this 2O+2Fe **B** motif is –131 kcal/mol (see Fig. S3 in SI). This indicates that the **M** binding motif is more favourable than the 2O+2Fe **B** one at the 100 goethite surface plane.

3.3.3. Outer–sphere complex formation

The possibility of outer–sphere complex formation between GLP and the 100 goethite surface has been studied by introducing GLP at the surface without direct covalent bond between them. Upon equilibration, two protons have been transferred from GLP to the surrounding water molecules. Furthermore, formation of two **M** covalent bonds between water and goethite and intermolecular water–goethite HBs have been observed. In fact, there is an indirect interaction between GLP and the goethite surface in which water acts as a bridge (see Fig. 3h). The calculated average interaction energy

between GLP and the goethite surface is –43 kcal/mol (see Fig. S3 in SI).

3.4. Effect of water

In this section, we will focus on the effect of water as a solvent for the real environmental molecular systems. Here, all the MD simulations have been performed with the same previous modeling setup in vacuum, i.e. without water. Four main points will be briefly introduced including 1- the competition between water and goethite regarding their interaction with GLP, 2- the competition between GLP and water regarding their interaction with the goethite surface, 3- the pH effect, and 4- the stability of the previously discussed binding motifs in the absence of water.

First, we focus on the competition between water and goethite regarding their interaction with GLP. To achieve this goal, exemplary MD simulations have been performed for the same starting configuration as for the **M** complex between GLP and the 010 goethite surface plane (see Fig. 2e) but without including water. As a result, one observes a very strong interaction between GLP and goethite. Snapshots along the MD trajectory are shown in Fig. 4. Here, GLP approaches to the surface with its carboxylic acid group, leading to a situation where GLP interacts through both its carboxylic and phosphonic groups. This gives rise to formation of three HBs (two from the phosphonic and one from the carboxylic group) and one **M** Fe–O bond (see Fig. 4d). Comparing with the situation in the presence of water (see Fig. 3a) we notice that, apparently, water retards the interaction between GLP and the goethite surface and competes with the surface regarding their interactions with GLP. This indicates the possibility of the GLP carboxylic group interaction with the surface in the absence of water. Finally, one can predict that solvation of the carboxylic group is more preferable than formation of a surface bond in the presence of water.

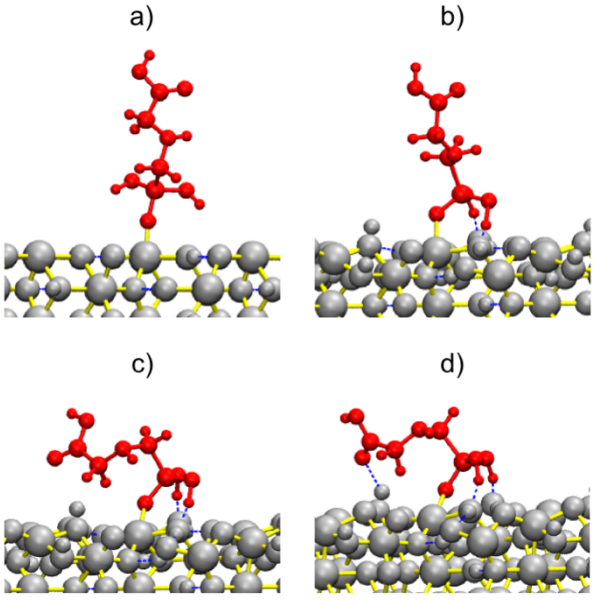

Figure 4. Four snapshots, from a) to d), characterizing the interaction of GLP with goethite surface in vacuum along the MD trajectory representing the GLP approach to the 010 goethite surface with its carboxylic acid group. The first given snapshot a) corresponds to the initial configuration of the GLP **M** binding motif at the 010 goethite surface.

Second, a more detailed view of the GLP and water interactions with the goethite surface is obtained by focussing on a single GLP as well as a single water molecule at the bare 010 goethite surface. Geometry optimization has been performed in vacuum for both cases. The obtained optimized geometries are shown in Fig. 5a-b. The calculated interaction energies for GLP and water with goethite are –53 and –31 kcal/mol, respectively. This indicates that GLP indeed binds stronger than water to goethite and explains why GLP can easily exchange the water molecules at the goethite surface. In passing we note that the difference with respect to the MD results can be explained by the formation of a dissociative **M** binding motif (Fig. 3a) in the MD case. This can increase the interaction energy two times or more compared to a non-dissociative binding motif (Fig. 5a), that agrees with previous studies.[45]

Third, we discuss the effect of the soil solution pH. To get an estimate of the associated interaction energies, the effect of high pH has been simulated by geometry optimization of a setup where a single OH^- group, in the presence of K^+ as counter ion, forms a **M** binding motif with the 010 goethite surface (Fig. 5c). The resulting interaction energy between the OH^- group and goethite was –80 kcal/mol, thus indicating a stronger adsorption for OH^- than GLP at the goethite surface. This means that at high pH, OH^- can replace the adsorbed GLP at the goethite surface yielding a strong drop of the GLP adsorption. This explains at a molecular level the experimental results referring to the GLP adsorption decrease with increasing the soil solution pH.[23,24,46] Of course, the absolute numbers of this comparison in gas phase should be taken with caution and cannot be used for solution phase estimates.

Finally, to elucidate the decisive role played by water as the solvating medium, the six GLP–goethite models without water have been investigated using quantum chemical geometry optimization. The optimized structures for all models are gathered in Fig. 5 (a, and d-h). For more details, relevant important bond lengths are summarized in Tab. S1. Here we will compare briefly the structural differences to the GLP–goethite–water models. In general, approach of the GLP carboxylic group to the goethite surface and their direct interaction has been observed for most cases, which is in contrast to the models including water (for details, see Fig. 5d and 5f-h). In addition to the covalent bond formation between GLP and the different goethite surface planes, several intermolecular HBs have been observed for all cases (see Fig. 5a,d-h). Moreover, proton transfer processes have been found from GLP to the 001 and 100 goethite surfaces (see Fig. 5e-h). The 010 goethite surface exhibits the same binding motifs (**M** and 2O+1Fe **B**) like to the case of including water. Similarly, the 100 goethite surface also exhibits the same binding motifs (**M** and 2O+2Fe **B**) as the case of including water. For the 001 goethite surface, two different stable **B** binding motifs (1O+2Fe and 2O+2Fe) have been formed between GLP and the surface. This indicates the stability of the 2O+2Fe **B** binding motif and the instability of the **M** one at the 001 goethite in vacuum compared to the case of including water.

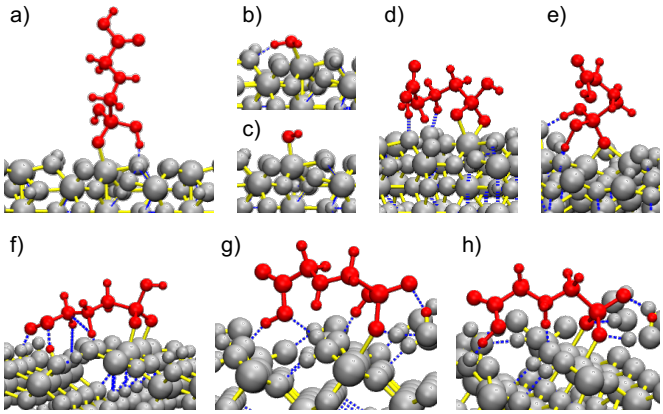

Figure 5. Vacuum geometry optimized structures for the GLP **M** motif (a), H_2O (b), OH^- (c), and GLP 2O+1Fe **B** motif (d) at the 010 goethite surface plane; GLP 1O+2Fe **B** motif (e) and GLP 2O+2Fe **B** motif (f) at the 001 goethite surface plane; and GLP **M** motif (g) and GLP 2O+2Fe **B** motif (h) at the 100 goethite surface plane.

4. Summarizing discussion and conclusions

There is a huge body of investigations discussing the GLP–goethite binding nature, formation of **M** versus **B** binding motif, and pH effect on this interaction with the aim to clarify the impact and fate of GLP in the environment. With a few exceptions, most of it is experimental work, which provides only indirect insight into the molecular level details. Direct insight comes from atomistic simulations, but the dynamics and mechanism of the overall GLP–goethite–water interactions and the individual GLP–goethite, GLP–water, and goethite–water interactions for different goethite surface planes have not yet been explored at the molecular scale. This gap has been filled by the present contribution, which aimed to investigate the mechanism and dynamics of the different GLP binding motifs at different goethite surface planes, intermolecular as well as intramolecular HBs, the competition between GLP and water molecules for goethite adsorption sites, effect of solution pH, and effect of water. For the first time, these objectives have been tackled using DFT-based MD ab initio simulations. The main results can be summarized as follows:

For all GLP–goethite models, MD simulations showed that neither the GLP amino group nor the carboxylic one contributes to the surface complexation, which is in good agreement with previous studies.[23,24] In addition, GLP was found to be stable against dissociation of its C–N and C–P bonds (their calculated distances vary in the range of 1.46–1.49 and 1.83–1.85 Å, respectively), which is in accord with experimental data indicating that these GLP bonds are highly stable and impervious to strong acid/base hydrolysis.[47]

Referring to the heterogeneity of goethite nanoparticles in real environmental systems containing different crystal planes, two binding motifs have been examined for the considered relevant crystal planes. They all exhibit **M** binding motifs and their binding stability to the goethite surface planes increases in the order 001 < 010 < 100 surface plane. Three stable **B** binding motifs have been investigated for the different surface planes with a binding stability increases in the order 2O+2Fe **B** at the 100 surface < 1O+2Fe **B** at the 001 surface < 2O+1Fe **B** at the 010 surface. Overall, the binding strength of GLP at the goethite surface increase in the order **M** at 001 < **M** at 010 < **B** at 100 < **M** at 100 < **B** at 001 < **B** at 010. Therefore, one can conclude that in general the binding motifs for GLP at the 010 goethite surface plane are more favoured than the corresponding ones at the 001 surface plane. This indicates to stronger binding for GLP at the 010 surface plane compared to the 001 surface plane. Moreover, both the 010 and 001 goethite surface planes prefer formation of the **B** binding motif to the **M** one. In contrast, the **M** binding motif is more favoured than the **B** one at the 100 surface. In addition, this **M** binding motif is more favourable than the corresponding ones at the 010 and 001 surface planes. One may attribute this observation to the saturation of the Fe atom participating in the **M** motif to its octahedral coordination for the 100 goethite surface plane, compared with the same **M** binding motifs at the 001 and 010 surfaces. Similarly, one can conclude that the **M** binding motif stability increases with increasing the coordination of its contributing Fe atom. This explains the increasing interaction energy between GLP and goethite for the **M** binding motifs at the goethite surface in the order of 001 < 010 < 100 surface plane.

The present study indicates that the most stable **M** and **B** binding motif occurs for the 100 and 010 goethite surface planes, respectively. Considering the fact that the 100 surface plane is the most abundant surface plane, one can conclude that the **M** binding motif is the most predominant species for the GLP adsorption on goethite. This is in good agreement with previous experimental[23] and theoretical[26] studies referring to the predominance of the **M** binding motif compared with the **B** one.

GLP forms dissociative complexes with the studied goethite surfaces by deprotonation and transfer of these protons to the surrounding water as well as to the surface. This process increases the interaction energies between GLP and the relevant surfaces as discussed in Ref.[45]. For most cases, some of the transferred protons stayed in contact with their original GLP donating O atoms via HB formation. The presence of these HBs between the GLP phosphonate group and the goethite surface enhances formation of the **M** binding motifs over the **B** one. The same effect has also been observed due to formation of intramolecular HB between the GLP phosphonate and amino groups. This confirms and explains the experimental outcomes by Sheals et al.[23] indicating that GLP adsorbs via predominantly **M** complexation in the presence of this intramolecular HB between the GLP phosphonate and amino groups. In addition, considering the fact that the GLP deprotonation process takes place with increasing the solution pH, one can explain the predominance of the **M** binding motif at low pH and the predominance of the **B** one by increasing the pH up to around the neutral pH as found in Refs. [23,24].

In addition to the strong interaction between GLP and the goethite surface, water also shows a strong interaction with the goethite surface. This interaction included formation of **M** and

also **B** motifs between the water O atoms and the surface Fe atoms of different surface planes, dissociation of water at the surface, and formation of intermolecular HBs between water and the surface. But in comparison with the GLP–goethite–interaction, our results indicate that GLP can replace the competing water molecules at the goethite surface. In the same context, we have found that the presence of the OH^- can replace the adsorbed GLP at the goethite surface. This is a key point for explaining the experimental observation of the drastic drop in the GLP adsorption at high pH.[23,24,46]

To summarize, we have provided a molecular-level picture of the various interactions occurring at the goethite-water interface in the presence of GLP. The explicit consideration of water molecules has been found to be vital for any realistic simulation of GLP binding. The present exhaustive study of different binding motifs and surface planes using ab initio molecular dynamics will provide a benchmark and starting point for future investigations of the interactions of GLP and other phosphorus-containing compounds with soil constituents.

Conflicts of interest

There are no conflicts to declare.

Acknowledgement

This work belongs to the InnoSoilPhos-project, funded by the German Federal Ministry of Education and Research (BMBF) in the frame of the BonaRes-program (No. 031A558). This research was performed within the scope of the Leibniz ScienceCampus “Phosphorus Research” Rostock.

References

1 Guyton, K. Z.; Loomis, D.; Grosse, Y.; El Ghissassi, F.; Benbrahim-Tallaa, L.; Guha, N.; Scoccianti, C.; Mattock, H.; Straif, K. Carcinogenicity of Tetrachlorvinphos, Parathion, Malathion, Diazinon, and Glyphosate. *Lancet Oncol.* **2015**, *16* (5), 490–491.

2 Myers, J. P.; Antoniou, M. N.; Blumberg, B.; Carroll, L.; Colborn, T.; Everett, L. G.; Hansen, M.; Landrigan, P. J.; Lanphear, B. P.; Mesnage, R.; Vandenberg, L. N.; vom Saal, F. S.; Welshons, W. V.; Benbrook, C. M. Concerns over Use of Glyphosate-Based Herbicides and Risks Associated with Exposures: A Consensus Statement. *Environ. Health* **2016**, *15* (1).

3 Coupe, R. H.; Kalkhoff, S. J.; Capel, P. D.; Gregoire, C. Fate and Transport of Glyphosate and Aminomethylphosphonic Acid in Surface Waters of Agricultural Basins. *Pest Manag. Sci.* **2012**, *68* (1), 16–30.

4 Van Stempvoort, D. R.; Roy, J. W.; Brown, S. J.; Bickerton, G. Residues of the Herbicide Glyphosate in Riparian Groundwater in Urban Catchments. *Chemosphere* **2014**, *95*, 455–463.

5 Skeff, W.; Neumann, C.; Schulz-Bull, D. E. Glyphosate and AMPA in the Estuaries of the Baltic Sea Method Optimization and Field Study. *Mar. Pollut. Bull.* **2015**, *100* (1), 577–585.

6 Khoury, G. A.; Gehris, T. C.; Tribe, L.; Torres Sánchez, R. M.; dos Santos Afonso, M. Glyphosate Adsorption on Montmorillonite: An Experimental and Theoretical Study of Surface Complexes. *Appl. Clay Sci.* **2010**, *50* (2), 167–175.

7 Liu, B.; Dong, L.; Yu, Q.; Li, X.; Wu, F.; Tan, Z.; Luo, S. Thermodynamic Study on the Protonation Reactions of Glyphosate in Aqueous Solution: Potentiometry, Calorimetry and NMR Spectroscopy. *J. Phys. Chem. B* **2016**, *120* (9), 2132–2137.

8 Hance, R. J. Adsorption of Glyphosate by Soils. *Pestic. Sci.* **1976**, *7* (4), 363–366.

9 Carlisle, S. M.; Trevors, J. T. Glyphosate in the Environment. *Water. Air. Soil Pollut.* **1988**, *39* (3), 409–420.

10 McBride, M. B. Electron Spin Resonance Study of Copper Ion Complexation by Glyphosate and Related Ligands. *Soil Sci. Soc. Am. J.* **1991**, *55* (4), 979.

11 Albers, C. N.; Banta, G. T.; Hansen, P. E.; Jacobsen, O. S. The Influence of Organic Matter on Sorption and Fate of Glyphosate in Soil – Comparing Different Soils and Humic Substances. *Environ. Pollut.* **2009**, *157* (10), 2865–2870.

12 Gros, P.; Ahmed, A.; Kühn, O.; Leinweber, P. Glyphosate Binding in Soil as Revealed by Sorption Experiments and Quantum-Chemical Modeling. *Sci. Total Environ.* **2017**, *586*, 527–535.

13 Piccolo, A.; Celano, G.; Arienzo, M.; Mirabella, A. Adsorption and Desorption of Glyphosate in Some European Soils. *J. Environ. Sci. Health Part B* **1994**, *29* (6), 1105–1115.

14 Hill, H. H. Competitive Sorption between Glyphosate and Inorganic Phosphate on Clay Minerals and Low Organic Matter Soils. *J. Radioanal. Nucl. Chem.* **2001**, *249* (2), 385–390.

15 Sprankle, P.; Meggitt, W. F.; Penner, D. Rapid Inactivation of Glyphosate in the Soil. *Weed Sci* **1975**, *23*, 224–228.

16 Glass, R. L. Metal Complex Formation by Glyphosate. *J. Agric. Food Chem.* **1984**, *32* (6), 1249–1253.

17 Dubbin, W. E. .; Sposito, G. .; Zavarin, M. . X-Ray Absorption Spectroscopic Study of Cu-Glyphosate Adsorbed by Microcrystalline Gibbsite. *Soil Sci.* **2000**, *165* (9), 699–707.

18 Nowack, B. Environmental Chemistry of Phosphonates. *Water Res.* **2003**, *37* (11), 2533–2546.

19 Jonsson, C. Modeling of glyphosate and metal-glyphosate speciation in solution and at solution-mineral interfaces, Department of Chemistry, Umeå Univ.: Umeå, 2007.

20 Ramstedt, M.; Norgren, C.; Shchukarev, A.; Sjöberg, S.; Persson, P. Co-Adsorption of cadmium(II) and Glyphosate at the Water–manganite (γ-MnOOH) Interface. *J. Colloid Interface Sci.* **2005**, *285* (2), 493–501.

21 McConnell, J. S.; Hossner, L. R. pH-Dependent Adsorption Isotherms of Glyphosate. *J. Agric. Food Chem.* **1985**, *33* (6), 1075–1078.

22 Day, G. M.; Hart, B. T.; McKelvie, I. D.; Beckett, R. Influence of Natural Organic Matter on the Sorption of Biocides onto Goethite, I. γ-BHC and Atrazine. *Environ. Technol.* **1997**, *18* (8), 769–779.

23 Sheals, J.; Sjöberg, S.; Persson, P. Adsorption of Glyphosate on Goethite: Molecular Characterization of Surface Complexes. *Environ. Sci. Technol.* **2002**, *36* (14), 3090–3095.

24 Barja, B. C.; dos Santos Afonso, M. Aminomethylphosphonic Acid and Glyphosate Adsorption onto Goethite: A Comparative Study. *Environ. Sci. Technol.* **2005**, *39* (2), 585–592.

25 Jonsson, C. M.; Persson, P.; Sjöberg, S.; Loring, J. S. Adsorption of Glyphosate on Goethite (α-FeOOH): Surface Complexation Modeling Combining Spectroscopic and Adsorption Data. *Environ. Sci. Technol.* **2008**, *42* (7), 2464–2469.

26 Tribe, L.; Kwon, K. D.; Trout, C. C.; Kubicki, J. D. Molecular Orbital Theory Study on Surface Complex Structures of Glyphosate on Goethite: Calculation of Vibrational Frequencies. *Environ. Sci. Technol.* **2006**, *40* (12), 3836–3841.

27 Xiu, F.; Zhou, L.; Xia, S.; Yu, L. Adsorption Mechanism of Water Molecule on Goethite (010) Surface. *J. Ocean Univ. China* **2016**, *15* (6), 1021–1026.

28 Guo, H.; Barnard, A. S. Thermodynamic Modelling of Nanomorphologies of Hematite and Goethite. *J. Mater. Chem.* **2011**, *21* (31), 11566.

29 Rakovan, J.; Becker, U.; Hochella, M. F. Aspects of Goethite Surface Microtopography, Structure, Chemistry, and Reactivity. *Am. Mineral.* **1999**, *84* (5–6), 884–894.

30 Cornell, R. M.; Schwertmann, U. *The Iron Oxides: Structure, Properties, Reactions, Occurrences, and Uses*, 2nd, completely rev. and extended ed ed.; Wiley-VCH: Weinheim, 2003.

31 Paul, K. W.; Kubicki, J. D.; Sparks, D. L. Sulphate Adsorption at the Fe (hydr)oxide–H2O Interface: Comparison of Cluster and Periodic Slab DFT Predictions. *Eur. J. Soil Sci.* **2007**, *58* (4), 978–988.

32 Kubicki, J. D.; Paul, K. W.; Sparks, D. L. Periodic Density Functional Theory Calculations of Bulk and the (010) Surface of Goethite. *Geochem. Trans.* **2008**, *9*, 4.

33 Kubicki, J. D.; Tunega, D.; Kraemer, S. A Density Functional Theory Investigation of Oxalate and Fe(II) Adsorption onto the (010) Goethite Surface with Implications for Ligand- and Reduction-Promoted Dissolution. *Chem. Geol.* **2017**, *464*, 14–22.

34 Szytuła, A.; Burewicz, A.; Dimitrijević, ž.; Kraśnicki, S.; Rżany, H.; Todorović, J.; Wanic, A.; Wolski, W. Neutron Diffraction Studies of α-FeOOH. *Phys. Status Solidi B* **1968**, *26* (2), 429–434.

35 Van Der Spoel, D.; Lindahl, E.; Hess, B.; Groenhof, G.; Mark, A. E.; Berendsen, H. J. C. GROMACS: Fast, Flexible, and Free. *J. Comput. Chem.* **2005**, *26* (16), 1701–1718.

36 VandeVondele, J.; Krack, M.; Mohamed, F.; Parrinello, M.; Chassaing, T.; Hutter, J. Quickstep: Fast and Accurate Density Functional Calculations Using a Mixed Gaussian and Plane Waves Approach. *Comput. Phys. Commun.* **2005**, *167* (2), 103–128.

37 Hutter, J.; Iannuzzi, M.; Schiffmann, F.; VandeVondele, J. CP2K: Atomistic Simulations of Condensed Matter Systems. *Wiley Interdiscip. Rev. Comput. Mol. Sci.* **2014**, *4* (1), 15–25.

38 Lippert, B. G.; Parrinello, J. H. and M. A Hybrid Gaussian and Plane Wave Density Functional Scheme. *Mol. Phys.* **1997**, *92* (3), 477–488.

39 Perdew, J. P.; Burke, K.; Ernzerhof, M. Generalized Gradient Approximation Made Simple. *Phys. Rev. Lett.* **1996**, *77* (18), 3865–3868.

40 Krack, M. Pseudopotentials for H to Kr Optimized for Gradient-Corrected Exchange-Correlation Functionals. *Theor. Chem. Acc.* **2005**, *114* (1–3), 145–152.

41 VandeVondele, J.; Hutter, J. Gaussian Basis Sets for Accurate Calculations on Molecular Systems in Gas and Condensed Phases. *J. Chem. Phys.* **2007**, *127* (11), 114105.

42 Grimme, S.; Ehrlich, S.; Goerigk, L. Effect of the Damping Function in Dispersion Corrected Density Functional Theory. *J. Comput. Chem.* **2011**, *32* (7), 1456–1465.

43 Jansen, H. B.; Ros, P. Non-Empirical Molecular Orbital Calculations on the Protonation of Carbon Monoxide. *Chem. Phys. Lett.* **1969**, *3* (3), 140–143.

44 Laage, D.; Hynes, J. T. A Molecular Jump Mechanism of Water Reorientation. *Science* **2006**, *311* (5762), 832.

45 Xiang, G.; Wang, Y.-G.; Li, J.; Zhuang, J.; Wang, X. Surface-Specific Interaction by Structure-Match Confined Pure High-Energy Facet of Unstable TiO2(B) Polymorph. *Sci. Rep.* **2013**, *3*.

46 Morillo, E.; Undabeytia, T.; Maqueda, C.; Ramos, A. Glyphosate Adsorption on Soils of Different Characteristics. *Chemosphere* **2000**, *40* (1), 103–107.

47 Jaisi, D. P.; Li, H.; Wallace, A. F.; Paudel, P.; Sun, M.; Balakrishna, A.; Lerch, R. N. Mechanisms of Bond Cleavage during Manganese Oxide and UV Degradation of Glyphosate: Results from Phosphate Oxygen Isotopes and Molecular Simulations. *J. Agric. Food Chem.* **2016**, *64* (45), 8474–8482.

Supplementary Information:

Unravelling the nature of glyphosate binding to goethite surfaces by ab initio molecular dynamics simulations

Ashour A. Ahmed[1,2,*], Peter Leinweber[3], Oliver Kühn[1]

[1] University of Rostock, Institute of Physics, D-18059 Rostock, Albert-Einstein-Str. 23-24, Germany.

[2] University of Cairo, Faculty of Science, Department of Chemistry, 12613 Giza, Egypt.

[3] University of Rostock, Soil Science, D-18059 Rostock, Germany.

ashour.ahmed@uni-rostock.de

peter.leinweber@uni-rostock.de

oliver.kuehn@uni-rostock.de

Figures

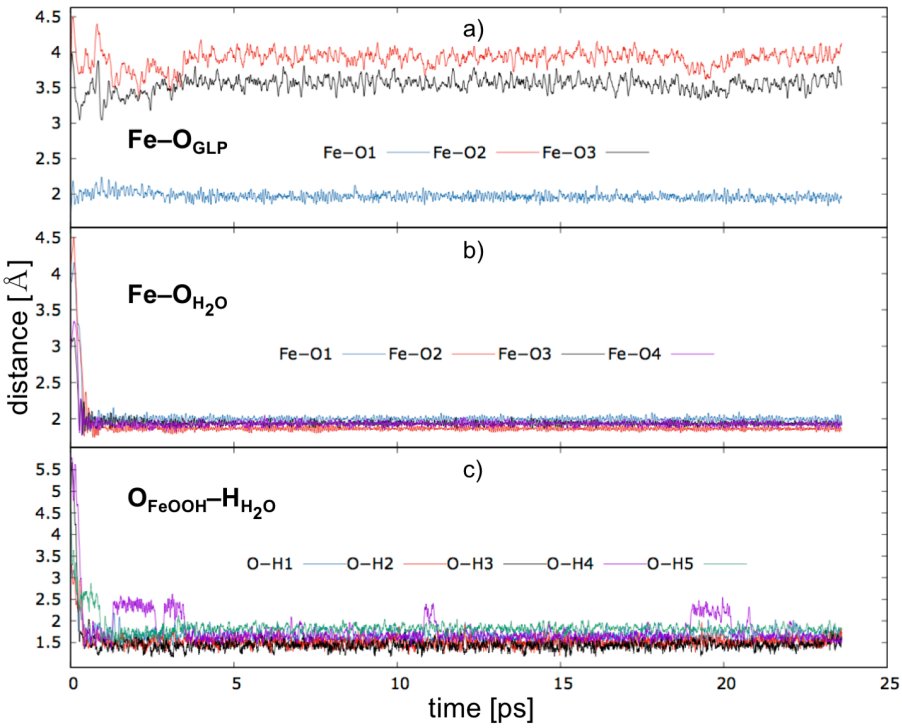

Figure S1. Intermolecular distance between the GLP phosphonate O atoms and surface Fe contributed to the monodentate binding motif (a), water O atoms and different surface Fe atoms (b), and water H atoms and different surface O atoms (c) along the MD trajectory of the monodentate binding motif at the 010 goethite surface plane.

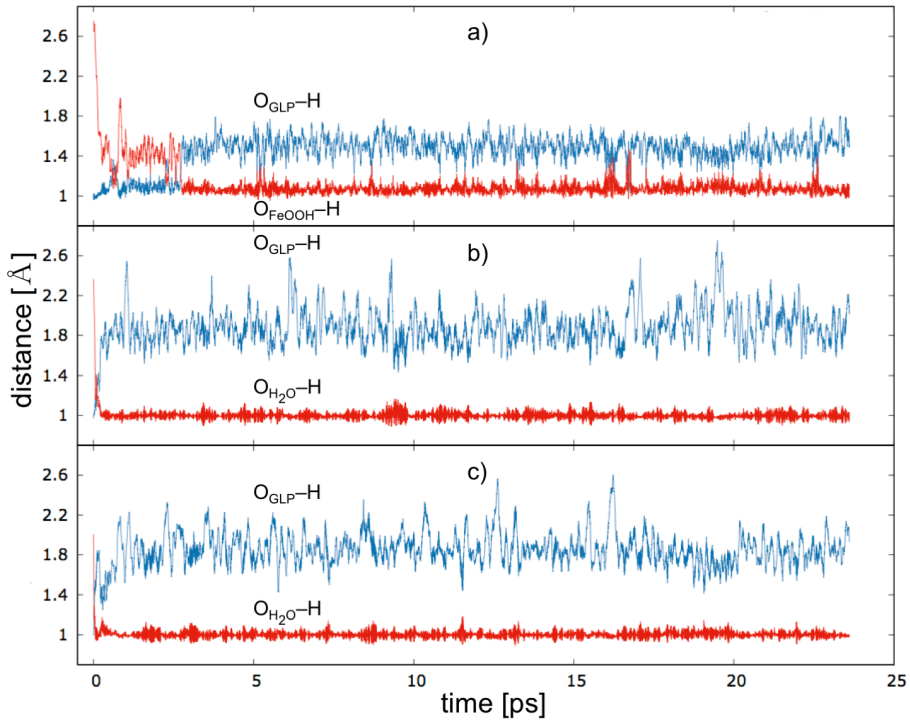

Figure S2. Intermolecular proton transfer from GLP to goethite surface (a), and water (b,c) along the MD trajectory of the monodentate binding motif at the 010 goethite surface plane.

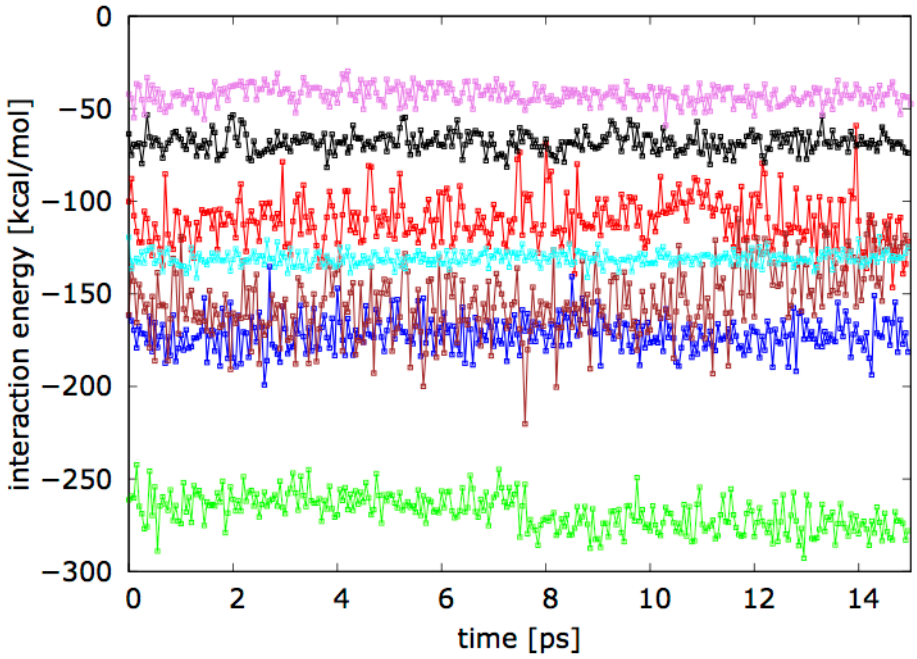

Figure S3. Interaction energy in kcal/mol along the production trajectory between GLP and the different goethite surface planes. Red, green, black, blue, brown, cyan, violet colours are corresponding to the monodentate at 010–, bidentate at 010–, monodentate at 001–, bidentate at 001–, monodentate at 100–, bidentate at 100–, and outer surface complex at 100–goethite surface plane, respectively.

Table

Table S1. Selected bond lengths in Å for the geometry optimized binding motifs at the 010, 001, and 100 goethite surface planes.

surface plane	binding motif	distance [Å]			
		C–N	C–P	$Fe_{goethite}$–O_{GLP}	Fe–P
010	monodentate	1.45	1.82	1.96	3.00
	bidentate (2O+1Fe)	1.49	1.83	2.02 & 2.05	2.52
001	bidentate (1O+2Fe)	1.45	1.84	1.89 & 1.99	2.99 & 3.47
	bidentate (2O+2Fe)	1.47	1.84	1.90 & 1.91	2.76 & 2.87
100	monodentate	1.45	1.83	2.08	3.51
	bidentate (2O+2Fe)	1.49	1.84	2.02 & 2.03	3.20 & 3.20